

# Minimising of electromagnetic torque ripple of reluctance stepper motor

**Streszczenie.** Reluktancyjne silniki krokowe są powszechnie wykorzystywane w wielu aplikacjach przemysłowych, jednakże ze względu na specyficzną budowę i niezrównoważone zasilanie faz silnika są one narażone na duże tętnienia momentu. To z kolei może spowodować duże wibracje na obciążeniu, szczególnie w systemach z elastycznymi elementami. Artykuł prezentuje modyfikację napięcia sterującego, uwzględniając wartości indukcyjności kolejno zasilanych faz silnika. Pole elektromagnetyczne modelu zostało rozwiązane metodą elementów skończonych.

**Abstract.** Reluctance stepper motors are commonly used in many cost-sensitive industrial and consumer applications, however they are affected by a large torque ripple, due to construction and phase unbalancing. This, in turn, may cause large vibrations on the load, especially in those systems with flexible elements. This research presents a technique of dynamics improvement by modification of voltage control signal of the variable reluctance stepper motor. The problem is solved by the electromagnetic field modeling using the time – stepping finite element method.

**Minimalizacja tętnień momentu elektromagnetycznego reluktancyjnego silnika krokowego.**

**Słowa kluczowe:** reluktancyjny silnik krokowy, tętnienia momentu, metoda elementów skończonych

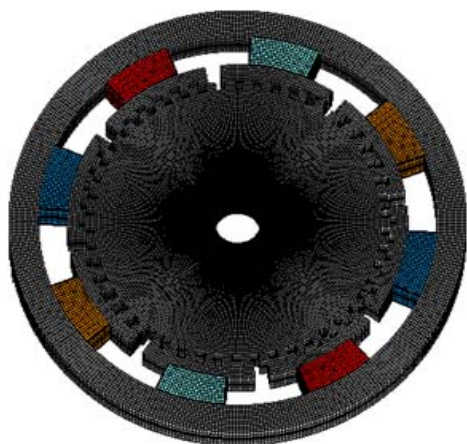
**Keywords:** reluctance stepper motor, torque ripple, finite element method

## Introduction

Reluctance stepper motors could achieve a very high resolution in positioning of mechanical loads, but torque ripple phenomenon is detrimental to the dynamics of the motor. It has been proposed many solutions with sensors signal feedback in order to solve this problem, however it is not always possible to accommodate a new position sensor on an existing mechanical system [1, 5,10]. This research presents a technique of dynamics improvement by modification of voltage control signal of the variable reluctance stepper motor. The authors present simulation results of reluctance stepper motors with a Torque Distribution Function in order to reduce torque ripple [1]. This control system can be easily fitted into existing systems, without any major modifications.

High performance motor drive applications require smooth torque with minimum torque ripple. This paper is focused on identifying voltage excitation associated with inductance functions on torque ripple. A modeling method and a numerical simulation of the two-phased unipolar variable reluctance stepper motor is presented (Figure 1).

Time stepping finite element approximation is applied to calculate the coupled field – circuit problem [2, 12]. Circuit equations are coupled with field equations creating one global system of non-symmetric equations. The mechanical motion of the rotor is determined by solving the second order differential motion equation. The magnetic torque is calculated by the Maxwell stress tensor [3, 4, 6].



— phase A — phase B — phase A' — phase B'

Fig. 1. Full 3D mesh of the reluctance stepper motor

Table 1. The main parameters of the reluctance stepper motor

motor parameters	Value [unit]
Nominal step $\theta_{nom}$	1.8 [degree]
Outer diameter of stator	39 [mm]
Inner diameter of stator	34 [mm]
Outer diameter of rotor	29.96 [mm]
Inner diameter of rotor	18 [mm]
Air gap width	0.02 [mm]
Motor length	30 [mm]
Rotor inertia	8.5 [gcm <sup>2</sup> ]
Friction	10 <sup>-5</sup> [Nms]

## Modeling technique

The electromagnetic device is fed by voltage sources. The equations that describe electric circuits is considered as [8]:

$$(1) \quad \frac{d}{dt} \oint_{l_1} \mathbf{A}(t) d\mathbf{l} = -R_1 i_1(t) + u_1(t)$$

$$(2) \quad \frac{d}{dt} \oint_{l_2} \mathbf{A}(t) d\mathbf{l} = -R_2 i_2(t) + u_2(t)$$

where:  $u(t)$  – represents coil voltage,  $R$  – coil resistance and  $i(t)$  – coil current. Equations that describe the magnetic field are constructed as the following boundary value problem [9]:

$$(3) \quad \int_{\Omega} \nabla \times \left( \frac{1}{\mu} \nabla \times \mathbf{A} \right) d\Omega = \int_{\Omega} \mathbf{j} d\Omega$$

Electric circuit equations (1) and (2) can be suitable coupled with field equations (3). This approach leads to construct a following system of linear equations:

$$(4) \quad \begin{bmatrix} \mathbf{C} & 0 & 0 \\ \frac{\mathbf{Q}_1}{\Delta t} & R_1 & 0 \\ \frac{\mathbf{Q}_2}{\Delta t} & 0 & R_2 \end{bmatrix} \begin{bmatrix} \mathbf{A}^{t+\Delta t} \\ i_1^{t+\Delta t} \\ i_2^{t+\Delta t} \end{bmatrix} = \begin{bmatrix} 0 \\ u_1^{t+\Delta t} + \frac{\mathbf{Q}_1}{\Delta t} \mathbf{A}^t \\ u_2^{t+\Delta t} + \frac{\mathbf{Q}_2}{\Delta t} \mathbf{A}^t \end{bmatrix}$$

The displacement of the rotor can be assumed as a one degree of freedom motion problem which is performed along axis  $\varphi$ .

$$(5) \quad \frac{d}{dt} \begin{bmatrix} \theta \\ \varphi \\ \omega \\ \varphi \end{bmatrix} = \begin{bmatrix} 0 & 1 \\ 0 & -\frac{b}{J} \end{bmatrix} \begin{bmatrix} \theta \\ \varphi \end{bmatrix} + \begin{bmatrix} 0 \\ \frac{1}{J} \end{bmatrix} M \varphi$$

where:  $J$  is a rotor inertia,  $b$  is a damping coefficient. The discrete form of the system of equations (5) is obtained using Eulers recurrence method.

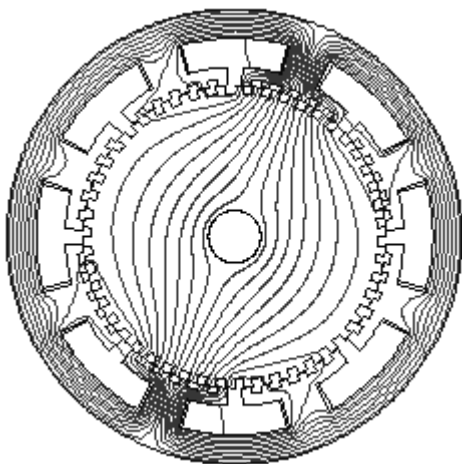


Fig. 2. Electromagnetic field distribution of the motor

At each time step, the global torque is calculated using the Maxwell stress method [3, 4, 6]. The force is evaluated along a surface in the air-gap around the rotor. The torque is obtained from the relationship:

$$(6) \quad \mathbf{T} = \oint_S \{ \mathbf{r} \times \mathbf{P} \} d\mathbf{S}$$

where:  $r$  is the position vector of the integration contour,  $P$  denotes the stress component defined around the rotor,  $dS$  is a surface segment.

Only z-component of the torque  $\mathbf{T} = [0 \ 0 \ T]^T$  is taken into consideration.

### Experiment

This approach to torque distribution is readily applicable to the model based on flux linkage due to the fact that there are no dynamics involved in the relationship between the phase currents and flux linkage.

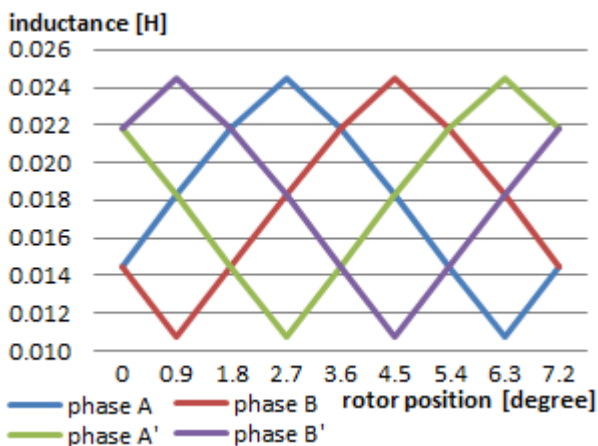


Fig. 3. Phase inductances in the analysed model

The data required for this procedure are the flux linkage versus stator excitation currents for discrete positions of the rotor. The inductance profiles of discussed motor has been

calculated in distributed parameters model and is shown in Figure 3.

In stepper motor control strategies, each phase winding is excited separately in the rising slope of the inductance for the positive torque, and in the falling slope for the negative torque (Figure 4) [11]. This approach has become the output for further analysis in this paper. The torque distribution as a function of time is presented in Figure 5.

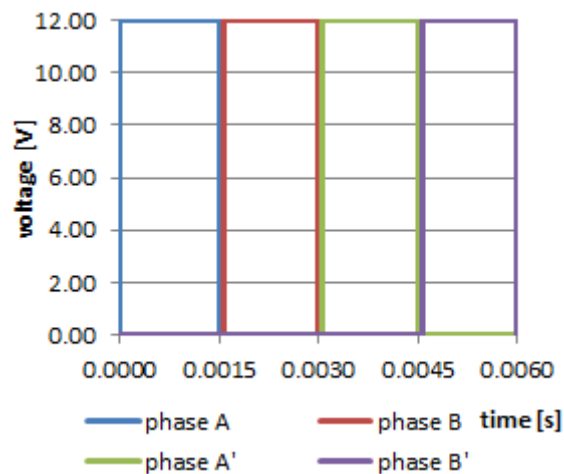


Fig. 4. Sequence voltage excitation of motor phases

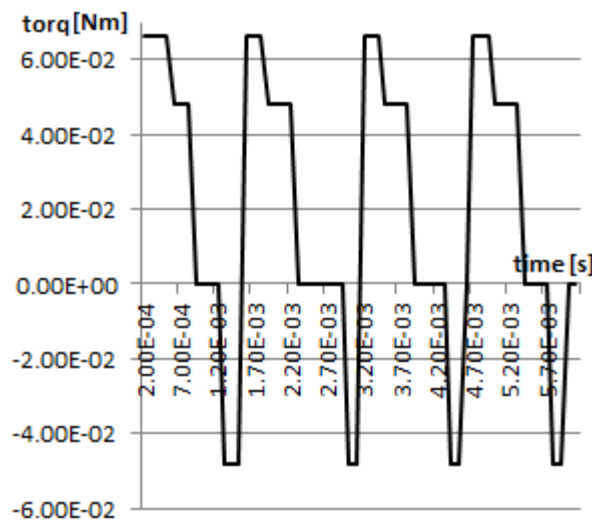


Fig. 5. Torque characteristic of stepper motor

During the commutation of one phase and initiation of another phase, the current flows in two phases. If the current is not controlled in the outgoing phase and only controlled in the incoming phase, the sum of the airgap torque contributed by only controlled in the incoming phase during this interval need not be a constant. The resultant torque usually has a through during this communication interval that increases the torque ripple [1].

A number of techniques have been presented in the literature to overcome some of the problems facing the torque control [1, 13]. In this paper the TDF method is used neglecting mutual inductance and saturation. Working based on these assumptions, the torque command will be divided into two parts, one for the incoming phase (phase x) and another for outgoing phase (phase y). The TDF III developed by Krishnan is used to calculate accurate phases excitations depended on inductances curves into torque communication interval. The total airgap torque can be

distributed to x and y, the two conducting phases of the machine [1].

$$(7) \quad T_e = T_x + T_y$$

$$(8) \quad T_x = \frac{1}{2} \frac{\partial L_x(\theta, i)}{\partial \theta} i_x^2 \quad \text{and} \quad T_y = \frac{1}{2} \frac{\partial L_y(\theta, i)}{\partial \theta} i_y^2$$

where:  $T_e$  – total torque,  $T_x$  – phase x torque,  $T_y$  – phase y torque,  $L_x$  – phase x inductance,  $L_y$  – phase y inductance,  $\theta$  – rotor position,  $i_x$  – phase x current,  $i_y$  – phase y current.

The voltage excitation function can be determined based on many criteria, such as: minimum peak current, minimum stator loss, minimum rotor displacement oscillations, etc [1, 11, 13].

In this paper the voltage excitation satisfying minimum torque ripple are determined by numerical method. The voltage excitation signal was modified in the interval of communication (Equation 9)

$$(9) \quad n\theta_{nom} + \delta \leq \theta \leq \left(n + \frac{1}{2}\right)\theta_{nom} + \delta$$

where:  $\theta_{nom}$  – nominal step (1.8 degree),  $\theta$  – actual rotor position,  $\delta$  – constant (offset depend on load),  $n \in \langle 1; 199 \rangle$

In ranges defined by Equation 9, the excitation has been calculated on the basis of a function of inductance power bands.

$$(10) \quad U_x = f_x * U_{nom} \quad \text{and} \quad U_y = f_y * U_{nom}$$

where:

$$(11) \quad f_x = \frac{\left(\frac{\partial L_x}{\partial \theta}\right)^2}{\left(\frac{\partial L_x}{\partial \theta}\right)^2 + \left(\frac{\partial L_y}{\partial \theta}\right)^2}, \quad f_y = \frac{\left(\frac{\partial L_y}{\partial \theta}\right)^2}{\left(\frac{\partial L_x}{\partial \theta}\right)^2 + \left(\frac{\partial L_y}{\partial \theta}\right)^2}$$

In this model of control excitation of succeeding coils reflects distribution of inductance (Figure 6 and Figure 3).

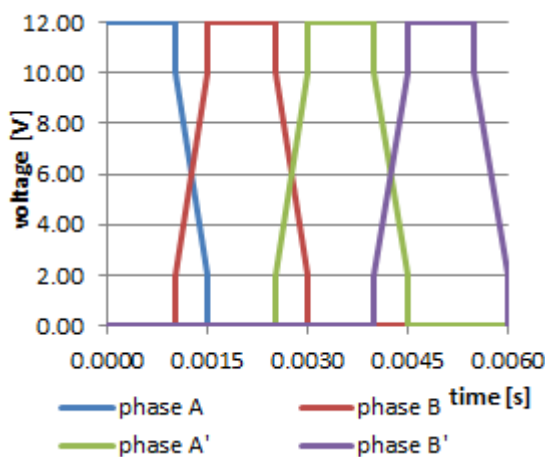


Fig. 6. Modified voltage excitations of motor phases

Rapid changes in the direction of the torque are detrimental to the dynamics of the motor step response. The approach presented in this paper has its justification in the case of high-speed control. Figure 8 presents displacements simulated for two cases: the classic

excitation (Figure 4) and the modified one with parameter  $\delta=0.3$  [degree]. The results show that torque ripple decrease caused a reduction in in motor displacement oscillations. It is worth emphasizing the fact that the proper selection of parameter  $\delta$  is crucial. If parameter  $\delta$  will be too small, then the motor will have worse dynamics. If, in turn, is too large, the reluctance stepper motor will have the momentary state of unstable.

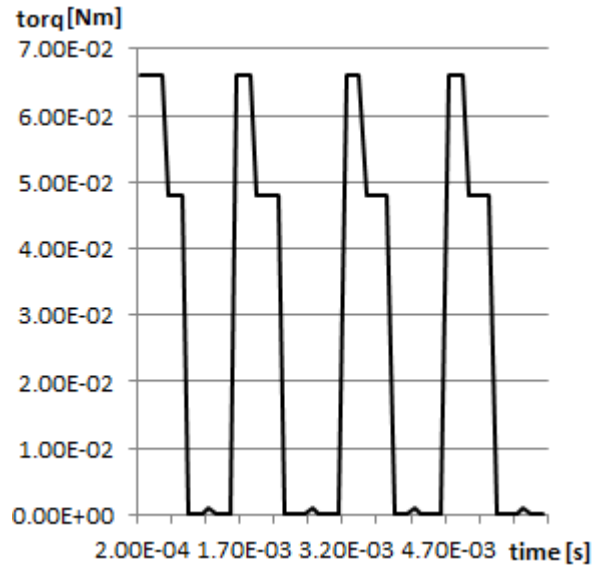


Fig. 7. Torque characteristic for modified model of control

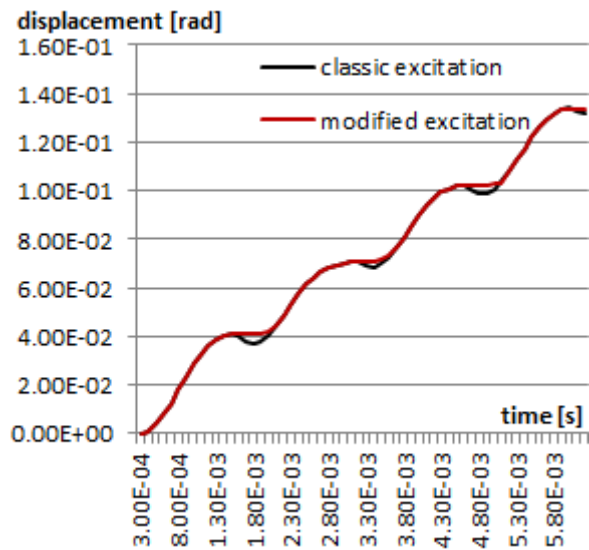


Fig. 8. Comparison of the rotor displacement characteristic

## Conclusions

There are various causes responsible for producing torque ripple in a reluctance stepper motor. The contributors of these undesirable effects may be categorized as those contributed from the motor and those from the electronic controller [1, 7]. This paper presented the theoretical analysis and numerical verification of a voltage drive control scheme for a two-phase unipolar reluctance stepper motor. For rectangular voltage excitations, it can be seen that the motoring torque is produced for a short duration in pulsed form, resulting in a large torque ripple. This can create problems of increased audible noise, fatigue of the shaft, and possible speed and displacement oscillations. The

torque ripples are minimized by designing the machine such that the inductance profiles of two succeeding phases overlap each other with a constant shift. An alternative technique to reduce torque ripple can be change the shape of the excitation in commutation interval. The model ignores saturation, so the inductances in the stepper motor phases are only depend on rotor position and not the excitation currents. The electromagnetic torque can then be calculated if the angular movement is known from the mechanical work. This approach works particularly when we want to achieve maximum motor speed in complying with the level of displacement oscillation.

#### REFERENCES

- [1] Krishnan R., Switched reluctance motor drives Modeling, Simulation, Analysis, Design, and Applications,(ser. I.E Boca Raton, FL; CRC Press, 2001)
- [2] Bernat J., Kołota J., Stępień S., Coupled field-motion model of variable reluctance stepper motor, *Electrical Review*, Vol.4 (2009), 210-213
- [3] Henrotte F., Handbook for the computation of electromagnetic forces in a continuous media, *ICS Newsletter*, Vol. 11(2004), No. 2, 10-17
- [4] Vijayakumar K., Karthikeyan R., Paramasivam S., Arumugam R., and Srinivas K., Switched Reluctance Motor Modeling, Design, Simulation, and Analysis: A Comprehensive Review, *IEEE Trans. Mag.*, Vol. 44 (2008), 4605-4617
- [5] Rahman K. M. and Schulz S. E., Design of high-efficiency and high torque density switched reluctance motor for vehicle propulsion, *IEEE Trans. Ind. Appl.*, Vol. 38 (2002), 1500–1507
- [6] Stępień S., Determination of electromagnetic torque with on-line computation of the optimal radius of the integration contour, *COMPEL* Vol. 29 (2010), 686-698
- [7] Bernat J., Kołota J., Stepien S., Dynamic of Reluctance Stepper Motor Depending on Different Air Gap, monograph: Information Systems Architecture and Technology – Model Based Decisions, 2008, pp. 179-191.
- [8] De Oliveira A., Antunes R., Kuo-Peng P., Sadowski N., Dular P. Electrical machine analysis considering field – circuit – movement and skewing effects, *Compel: The International Journal for Computation and Mathematics in Electrical and Electronic Engineering*, vol. 23 (2004), no. 4, pp. 1080-1091.
- [9] Stepien S., Patecki A., Modeling and Position Control of Voltage Forced Electromechanical Actuator, *Compel: The International Journal for Computation and Mathematics in Electrical and Electronic Engineering*, Vol. 25 (2006), No. 2, pp. 412-426.
- [10] Panda S.K., Xu J.X., Qian W., Review of torque ripple minimization in PM synchronous motor drives, *Power and Energy Society General Meeting – Conversion and Delivery of Electrical Energy in the 21st century*, July 2008, pp. 1-6.
- [11] Roux C., Morcos M. M., On the use of a simplified model for switched reluctance motors, *IEEE Trans. Energy Conv.* Vol. 17 (2002), pp.400-405.
- [12] Wu W., Dunlop J., Stephen B., Collocott J. and Kalan B., Design optimization of a switched reluctance motor by electromagnetic and thermal finite-element analysis, *IEEE Trans. Magn.* Vol. 39 (2003), 3334–3336
- [13] Schramm D.S., Williams B.W., Green T.C., Torque ripple reduction of switched reluctance motors by phase current optimal profiling, *IEEE Power Electronics Specialist Conf.*, 1992, pp. 857-860.

---

**Autorzy:** dr inż. Jakub Bernat, Poznan University of Technology, Chair of Computer Engineering, ul. Piotrowo 3a, 60-965 Poznan, E-mail: [Jakub.Bernat@put.poznan.pl](mailto:Jakub.Bernat@put.poznan.pl); dr inż. Jakub Kołota, Poznan University of Technology, Chair of Computer Engineering, ul. Piotrowo 3a, 60-965 Poznan, E-mail: [Jakub.Kolota@put.poznan.pl](mailto:Jakub.Kolota@put.poznan.pl); dr inż. Sławomir Stępień, Poznan University of Technology, Chair of Computer Engineering, ul. Piotrowo 3a, 60-965 Poznan, E-mail: [Slawomir.Stepien@put.poznan.pl](mailto:Slawomir.Stepien@put.poznan.pl).